Fluid Phase Equilibria 605 (2026) 114694

Contents lists available at ScienceDirect

Fluid Phase Equilibria

journal homepage: www.journals.elsevier.com/fluid-phase-equilibria

Vapor-liquid equilibrium for the separation of the n-hexane + ethanol azeotropic mixture with biobased entrainers guaiacol and dimethyl isosorbide

Dhoni Hartanto [a,b,*], Boelo Schuur [c], Anton A. Kiss [a], André B. de Haan [a]

[a] Department of Chemical Engineering, Delft University of Technology, Van der Maasweg 9, Delft, 2629 HZ, the Netherlands
[b] Department of Chemical Engineering, Faculty of Engineering, Universitas Negeri Semarang, Kampus Sekaran, Gunungpati, Semarang, 50229, Indonesia
[c] Sustainable Process Technology, Faculty of Science and Technology, University of Twente, Enschede, 7500 AE, the Netherlands

ARTICLE INFO

Keywords:
Extractive distillation
Azeotrope separation, green solvents
Biobased entrainers
Guaiacol
Dimethyl isosorbide
Vapor liquid equilibrium

ABSTRACT

In extractive distillation for the separation of azeotropic mixtures, eco-friendly solvents have demonstrated potential as greener alternatives to conventional entrainers. However, the absence of thermodynamic data for mixtures that include green solvents presents a significant hurdle to their practical application. This work explores, for the first time, vapor-liquid equilibrium (VLE) data for the azeotropic mixture of n-hexane and ethanol in the presence of the biobased entrainers guaiacol and dimethyl isosorbide (DMI). The VLE measurements were conducted using a Fischer Labodest VLE 502 ebulliometer with varying pressures and entrainer-to-feed ratios (E/Fs). The VLE data met the criteria of the Van Ness method and thereby pass the thermodynamic consistency test. The results confirm that the relative volatility of n-hexane to ethanol is increased by the addition of guaiacol and DMI to the mixture. Moreover, the azeotrope has been successfully removed. The VLE data were well regressed using the Non-Random Two Liquid (NRTL) thermodynamic model, which provided accurate binary interaction parameters (BIPs). The thermodynamic modeling verifies the reliability of the experimental data and its relevance for effective process design, emphasizing the viability of guaiacol and DMI as biobased entrainers for more sustainable and greener extractive distillation.

1. Introduction

Separation technologies play a central role in the process industry but encompass the most energy consuming and cost-intensive operations, contributing to more than half of the total energy usage and associated cost [1–3]. Moreover, separation processes, including distillation, account for an estimated 10–15 % of the total energy consumed worldwide [4]. A significant problem in these operations emerges in case an azeotrope is present in the mixture to be separated. The azeotropic point shares equal composition between vapor and liquid phases at particular temperature and pressure conditions due to non-ideal molecular interactions, which significantly complicates their separation. A notable example of such mixtures is n-hexane and ethanol, which is relevant across multiple sectors. This binary system commonly arises in petrochemical processes [5]. Ethanol, as one of the low-carbon alcohols, is generated from syngas derived from natural gas or coal. This direct syngas-to-ethanol pathway inherently produces C_{2+} hydrocarbons, including n-hexane [6,7]. Likewise, Fischer-Tropsch synthesis yields oxygenated compounds, including ethanol, together with hydrocarbons, such as n-hexane [8]. Since both n-hexane and ethanol are extensively used as solvents across a broad range of applications, achieving their effective separation is essential to obtain high purity of each component, considering the azeotrope inherent in the mixture [9].

In separation processes, distillation remains the predominant method due to its adaptability to various feed compositions and flow rates, effectiveness for complex mixture separation at industrial scale, and efficient operation and control, which deliver high-purity products across a diverse range of industrial applications. Furthermore, nearly every commercial product involving chemicals has been processed using distillation [10–12]. Currently, more than 100,000 distillation columns are operating globally, constituting a major share of both capital investment and operational expenditures [13,14].

Special distillation methods are needed to separate the azeotropic

* Corresponding author at: Department of Chemical Engineering, Delft University of Technology, Van der Maasweg 9, Delft, 2629 HZ, the Netherlands.
E-mail address: dhoni.hartanto@mail.unnes.ac.id (D. Hartanto).

https://doi.org/10.1016/j.fluid.2026.114694
Received 30 November 2025; Received in revised form 3 February 2026; Accepted 6 February 2026
Available online 7 February 2026

mixture since conventional distillation is unable to perform this separation. To address these limitations, more advanced approaches like extractive distillation are employed. In comparison with other separations methods, extractive distillation proves to be more efficient and reliable for use in various industries [15,16]. This method introduces a third separation agent, called an entrainer. The entrainer interacts with one of the components and therefore increases the relative volatility of the target component, allowing the separation to surpass azeotropic boundaries. In addition to enabling effective separation, extractive distillation offers environmental and economic advantages by reducing energy and water consumption, lowering cost, and decreasing CO_2 emissions.

Despite its promising potential for separating azeotropic mixtures, the frequent use of conventional entrainers like 1-methylpyrrolidin-2-one (NMP) hinders implementation of greener and more sustainable extractive distillation processes. NMP remains attractive due to its good polarity profile, high boiling point and thermal stability [17]. However, increasing concern over its health and ecological impacts has led chemical regulatory institutions, such as EPA from the U.S. and REACH from the E.U., to increasingly enforce limitations on these compounds [18,19]. As a result, there is an increasing need for greener entrainers that not only exhibit effective separation performance but also align with environmental and safety concerns.

Although interest in green solvents is rapidly growing, some of the promising biobased solvents, such as guaiacol and DMI, are overlooked as entrainers in extractive distillation. Moreover, there are no experimental VLE data and BIPs for n-hexane and ethanol with these solvents, which poses challenges for developing the process design. Thus, this research aims to fill that knowledge gap by providing the first VLE data for the n-hexane and ethanol mixture containing guaiacol and DMI.

In recent years, various green solvents have been examined as viable entrainers in extractive distillation for separating the close-boiling and azeotropic mixtures. Among them are biological buffers [20,21], biobased solvents [13,22–26], deep eutectic solvents and natural deep eutectic solvents (DESs and NADESs) [27–30], and ionic liquids (ILs) [31–34]. Recent studies on n-hexane and ethanol separation have identified various entrainers. Zhang et al. [35] reported the VLE data for the binary mixture of n-hexane and butyl propanoate and n-hexane + butyl butanoate. Additionally, Gonzalez and Ortega [36] studied the VLE data for the binary mixtures of ethanol + butyl propanoate and ethanol + butyl butanoate. However, these studies were limited to reporting only binary VLE data, and there is currently no experimental data available for the pseudo-ternary mixture involving n-hexane and ethanol in the presence of the entrainers butyl propanoate and butyl butanoate. Imidazolium-based ILs have been investigated as entrainers to separate n-hexane and ethanol. These ILs successfully eliminate the azeotropic point [37]. Sander et al. [38] investigated various DESs to overcome the azeotropic point in this mixture through extractive distillation experiments using a simple round-bottom flask. They discovered that menthol-decanoic acid and menthol-decanoic acid DESs are fully miscible. With the addition of a 0.05 mass fraction of these entrainers, the maximum n-hexane mass purity achieved was 0.87. However, other DESs, including choline chloride with glycerol, malic acid, citric acid, glycolic acid, and ethylene glycol, as well as lactic acid with glycerol, K_2CO_3 with glycerol and ethylene glycol, and tetramethylammonium chloride with glycolic acid, exhibited miscibility issues. In another report, glycerol-based DES is ineffective at separating the azeotrope in the n-hexane and ethanol mixture. Even with the addition of 30 % mass DES, the azeotrope remains in the mixture [39]. Although some ionic liquids and deep eutectic solvents exhibit promising entrainer performance in other azeotropic systems, their application to the n-hexane + ethanol mixture is often limited by high viscosity, complex synthesis routes, and miscibility constraints at high entrainer loadings. For example, several glycerol-based DESs cannot eliminate the n-hexane + ethanol azeotrope even at 30 mass % entrainer, and many show phase separation or composition-dependent immiscibility. Recent reports on DES-based entrainers for other azeotropes further emphasize that careful composition and temperature control is required to avoid phase separation and mass-transfer limitations, which complicate scale-up [29,38,39]. Furthermore, Wang et al. [40] reported the effect of several conventional solvents, including ethylene glycol, dimethyl sulfoxide, dimethylacetamide, 1,3-propanediol, dimethylformamide, 1, 2-propanediol, and NMP, on the separation of n-hexane and ethanol. This study is more focused on the evaluation of the extractive pressure-swing distillation process, and therefore complete experimental VLE data were not provided. The results indicate that all the solvents effectively break the azeotropic point in the n-hexane and ethanol mixture.

In contrast to NMP, which is classified as reprotoxic, guaiacol and DMI are not classified as reprotoxic, and exhibit substantially higher NOAEL (No Observed Adverse Effect Level) for DMI reflecting their lower developmental toxicity and better regulatory profile. NOAEL is the highest dose of exposure at which no adverse developmental effects are observed. A higher NOAEL value therefore indicates lower toxicity and, consequently, better chemical safety and greenness. Both are biodegradable and derived from renewable feedstocks, whereas NMP is petrochemical-based. These features provide a clear health and sustainability advantage, even if the thermodynamic separation performance is somewhat lower. Guaiacol is a non-reprotoxic chemical. Although no specific data on its developmental toxicity is available, its widespread use in the food, beverage, and pharmaceutical industries suggests that guaiacol presents a low reprotoxicity. DMI is also classified as low in reprotoxicity, with a NOAEL for developmental toxicity of 300 mg/kg body weight/day. Moreover, DMI has been recognized as one of the top ten biobased platform chemicals [41–46]. On the contrary, NMP is a reprotoxic solvent with the NOAEL of 160 mg/kg body weight/day [47]. This makes NMP unsuitable for industrial applications. Additionally, guaiacol (T_b=478.20 K) and DMI (T_b=513.15 K) were selected as they exhibit significantly higher boiling points than other biobased solvents, such as furfural (T_b=435.15 K), and provide better miscibility in hydrocarbons compared to glycerol derivatives.

Compared to NMP, these solvents have higher boiling points and comparable polarity, as indicated by Hansen Solubility Parameters (HSPs) [41,48–51]. Detailed information regarding their boiling point and HSPs is provided in Table S1 of the Supplementary Files. These properties make both entrainers advantageous for use in extractive distillation.

Given their promising solvent characteristics, guaiacol and DMI were selected for the VLE experimental in this study to assess their effectiveness in breaking the n-hexane – ethanol azeotrope. To ensure the reliability of the VLE data, thermodynamic consistency was verified using the Van Ness test [52]. Following this, data regression was performed to obtain the optimum BIPs using the NRTL model [53]. These results provide a robust thermodynamic foundation for the design and optimization of more eco-efficient extractive distillation involving guaiacol and DMI as green entrainers.

2. Experiments and methods

The subsequent sections provide the details of the chemical specifications, experimental apparatus, and methodology, along with the analytical techniques applied in this study.

2.1. Materials

All chemicals used in this study were obtained from commercial sources, and their purity was determined using gas chromatography (GC). The water content of hygroscopic compounds was measured using Karl Fischer (KF) titration (Metrohm-787 KF Titrino 703 TiStand, Switzerland). Due to the absence of substantial impurities, the chemicals were used as received without further purification. A detailed specification of these chemicals is summarized in Table 1.

Table 1
The detailed specification of the chemicals.

chemicals	CAS-No	MW (g/mol)	$T_{boiling}$ (K)[a,b]	density (g/cm^3)[a,c]	sources	purity (in a mass fraction)[a]	Water content (%)[d]	purity analysis	additional purification
n-hexane	110–54–3	86.18	342.15	0.660	Merck	≥0.990	-	GC[e]	none
ethanol	64–17–5	46.07	351.44	0.790	Merck	≥0.999	0.04	GC[e]	none
guaiacol	90–05–1	124.14	478.20	1.129	Acros Organics	≥0.990	0.07	GC[e]	none
dimethyl isosorbide	5306–85–4	174.20	513.15	1.167	Sigma-Aldrich	≥0.990	0.09	GC[e]	none
acetone	67–64–1	58.08	329.15	0.791	Merck	≥0.998	0.05	GC[e]	none

[a] specified by the suppliers;.
[b] pressure:101.3 kPa;.
[c] temperature: 298.15 and pressure: 101.3 kPa;.
[d] KF (Karl Fischer titration);.
[e] GC (gas chromatography).

2.2. Experimental details and procedures

The measurements of the VLE data for the investigated mixtures were performed using an ebulliometer (Fischer Labodest model VLE602, Germany). The temperature and pressure uncertainties of the setup, as reported by the company, are ±0.01 K and ±0.01 kPa. The schematic of the setup was illustrated by Dias et al. [54]. Freshly prepared mixtures and entrainers were precisely weighed using an analytical balance (Mettler Toledo AE200, USA). The uncertainty of this equipment is ±0.0001 g. Each mixture, with a volume of 100 mL, was charged into the ebulliometer for each experimental run to assure stable vapor and liquid phase circulation. For the vacuum experiments, a vacuum pump (Pfeiffer DUO 3, Germany) was employed. The vacuum conditions were regulated in a closed system using a pressure controller (Burkert 2871, Germany). Both the vacuum pump and a pressure controller were connected to the i-Fischer Unicontrol VLE digital interface, allowing for an accurate digital setting of the desired pressure. Throughout the experimental run, the pressure was consistently maintained.

The system was considered to have reached equilibrium once the temperature as well as the pressure remained steady within ±0.4 K and ±0.1 kPa. After 30 min, the temperature became constant, and another 30 min was applied to guarantee the equilibrium prior to sampling. This resulted in an overall experimental duration of 60 min. Consistent heating and temperature homogeneity in the system were ensured by employing a heating rod submerged in the liquid chamber, along with a heating mantle wrapped around the vapor chamber. To mitigate heat loss, the setup was enclosed with thermal insulation. Throughout the experiment, a magnetic stirrer operated continuously to maintain uniform mixing of the mixture. Furthermore, the condensed vapor was recirculated back to the liquid chamber as reflux, promoting proper circulation and temperature uniformity in the setup. These procedures ensured temperature stability and uniformity throughout the experiment.

Under equilibrium conditions, approximately 0.1 mL each of liquid and vapor condensate were sampled. Liquid samples were taken through a valve, while vapor samples were collected using a syringe. Every sample was quickly diluted in 1 mL of high-purity acetone before composition analysis by GC. The adopted experimental procedure is consistent with methods used in previous literature [13,22,23,55].

2.3. Analytical procedures

The analysis of the liquid and vapor phase compositions was conducted using a GC (Thermo Scientific Trace 1300 Series, Switzerland), configured with two parallel ovens and an automated TriPlus 100 liquid sampling unit. To facilitate compound separation, a capillary column of the Agilent DB-1MS (length: 60 m, diameter: 0.25 mm, film thickness: 0.25 μm) was used. Injections were performed in Split/Splitless (SSL) mode, with a sample injection volume of 1 μL.

The oven temperature profile was programmed in multiple ramping stages. It commenced at 30 °C and increased sequentially at 10 °C/min to reach 45 °C, then 5 °C/min to 60 °C, followed by an increase of 2.5 °C/min to 80 °C. Subsequently, the temperature increased at 5 °C/min to 95 °C, concluding with a rapid increase ramp of 50 °C/min up to 320 °C. This process was completed in 21 min. The detection of the compound was carried out using a Flame Ionization Detector (FID) operated at 440 °C. Helium served as the carrier gas, operating at 213.2 kPa, with a 2 mL/min column flow rate. A split injection was performed at 300 mL/min with a split ratio of 150, supplemented by hydrogen at a flow rate of 50 mL/min, air at flow rate 350 mL/min, and helium at a flow rate of 40 mL/min.

Standard mixtures with precisely known compositions were utilized to perform calibration prior to sample analysis. GC area fractions were plotted against the corresponding mole fractions of the standards to establish a regression equation. This equation was then used to calculate the mole fractions of the components in the samples based on their measured area responses. Analytical precision was maintained by conducting three replicate analyses per sample. This approach ensured analytical accuracy and reduced the potential impact of the methodological errors in the analysis. The final compositions are expressed as the mean value from these analyses. The standard uncertainties for pressure, temperature, and phase compositions were quantified following the methodologies outlined in the guidelines from NIST and JCGM [56,57], with equations provided in the Supplementary Files (Eqs. S1-S3). These uncertainty values are included with the VLE data presented in Section 3.1.

3. Results and discussion

3.1. Experimental results

Our previous studies have verified the reliability of both the setup and methods applied in this work [13,58]. The present study assessed the introduction of biobased entrainers guaiacol and DMI to the n-hexane and ethanol mixtures. The experimental VLE data for pseudo-ternary mixtures of n-hexane and ethanol involving guaiacol and DMI were measured. Each pseudo-ternary mixture was investigated at an E/F of 1 under the pressures of 50.0 kPa and 100.0 kPa and at an E/F of 3 at a pressure of 50.0 kPa. The E/F represents the amount of the entrainer introduced to the azeotropic mixture, which is defined as the mass of the entrainer divided by the mass of the azeotropic mixture. In all composition ranges of n-hexane examined under specified E/Fs and pressures, the presence of guaiacol and DMI in the n-hexane and ethanol mixture exhibit homogeneous mixtures, indicating that VLE measurements were feasible. Moreover, given that the laboratory pressure varied between 100 and 101.3 kPa, the experiments were conducted at 100.0 kPa in a closed vacuum system because it provided a more accurate pressure regulation in the setup.

The experimental VLE data for the pseudo-ternary mixture of n-hexane and toluene with guaiacol are provided in Table 2, while the data for the mixture with DMI are shown in Table 4. In these tables, x_1' and y_1' represent the entrainer-free mole fraction of liquid and vapor phases for n-hexane. The x_1, x_2, and x_3 denote the mole fractions of the liquid phase for n-hexane, ethanol, and entrainer, respectively, while y_1, y_2, and y_3 represent the mole fractions of the vapor phase for n-hexane, ethanol, and entrainer, respectively. The T, γ_1, γ_2, and α_{12} express the equilibrium temperature, the activity coefficient of n-hexane, the activity coefficient of ethanol, and the relative volatility of n-hexane to toluene, respectively. Since the absence of detectable entrainer in the vapor phase, y_3 is considered to be below 0.0005. Consequently, y_1' is regarded as equivalent to y_1. This threshold corresponds to the value that does not alter the activity coefficient or relative volatilities within the experimental uncertainty. To ensure consistency in reporting, the y_3 values are presented as 0.000 in Tables 2 and 4.

Eq. (1) defines the activity coefficient (γ_i), which was utilized to evaluate the non-ideal behavior of component i in the liquid phase of the pseudo-ternary mixtures. The vapor phase was treated as ideal, which is justified by the vacuum and atmospheric operating pressures under which the VLE experiments were conducted.

$$\gamma_i = \frac{y_i P}{x_i P_i^{sat}} \tag{1}$$

In this equation, x_i and y_i correspond to the mole fractions of component i in the liquid and vapor phase, respectively. P and P_i^{sat} refer to the total pressure in the system and the saturated vapor pressure of component i, respectively. The saturated vapor pressure was determined using equations and parameters from the extended Antoine and the NIST Wagner 25, which are taken from the Aspen Plus physical properties database. For n-hexane, ethanol, and guaiacol, the extended Antoine equation was employed. For DMI, the NIST Wagner 25 equation was applied since no data was available for the extended Antoine equation. The equations and their parameters are provided in Table 3.

Separation performance of the entrainer was examined using the relative volatility equation, as shown in Eq. (2).

Table 2
Experimental VLE data for pseudo-ternary mixture of n-hexane (1) + ethanol (2) + guaiacol (3)[a,b,c].

T/K	x_1'	x_1	x_2	x_3	y_1'	y_1	y_2	y_3	γ_1	γ_2	α_{12}
E/F = 1; 100.0 kPa											
358.65	0.000	0.000	0.729	0.271	0.000	0.000	1.000	0.000		1.026	
353.05	0.028	0.020	0.704	0.276	0.176	0.176	0.824	0.000	6.150	1.084	7.47
345.55	0.107	0.076	0.635	0.289	0.451	0.451	0.549	0.000	5.220	1.082	6.85
342.05	0.133	0.094	0.614	0.292	0.556	0.556	0.444	0.000	5.820	1.048	8.19
339.85	0.197	0.137	0.560	0.303	0.636	0.636	0.364	0.000	4.886	1.031	7.15
338.85	0.236	0.163	0.528	0.309	0.681	0.681	0.319	0.000	4.537	1.003	6.91
338.25	0.277	0.190	0.495	0.315	0.700	0.700	0.300	0.000	4.087	1.029	6.11
337.85	0.372	0.250	0.420	0.330	0.709	0.709	0.291	0.000	3.174	1.200	4.10
337.65	0.437	0.290	0.371	0.339	0.736	0.736	0.264	0.000	2.866	1.242	3.58
337.65	0.586	0.376	0.265	0.359	0.753	0.753	0.247	0.000	2.260	1.629	2.15
337.55	0.640	0.406	0.228	0.366	0.776	0.776	0.224	0.000	2.166	1.720	1.95
337.95	0.689	0.432	0.195	0.373	0.807	0.807	0.193	0.000	2.086	1.706	1.88
340.55	0.840	0.512	0.097	0.391	0.893	0.893	0.107	0.000	1.796	1.698	1.60
344.85	0.916	0.549	0.051	0.400	0.948	0.948	0.052	0.000	1.555	1.312	1.69
348.25	1.000	0.590	0.000	0.410	1.000	1.000	0.000	0.000	1.377		
E/F = 1; 50.0 kPa											
341.05	0.000	0.000	0.729	0.271	0.000	0.000	1.000	0.000		1.035	
334.35	0.027	0.019	0.705	0.276	0.238	0.238	0.762	0.000	7.706	1.089	11.40
325.05	0.113	0.080	0.630	0.290	0.560	0.560	0.440	0.000	6.015	1.078	10.00
322.15	0.140	0.099	0.607	0.294	0.654	0.654	0.346	0.000	6.329	1.009	11.65
320.05	0.214	0.148	0.546	0.306	0.722	0.722	0.278	0.000	5.017	0.998	9.58
318.75	0.270	0.185	0.500	0.315	0.749	0.749	0.251	0.000	4.370	1.049	8.07
318.25	0.342	0.231	0.444	0.325	0.770	0.770	0.230	0.000	3.675	1.110	6.45
318.25	0.421	0.279	0.384	0.337	0.795	0.795	0.205	0.000	3.134	1.146	5.33
318.15	0.424	0.281	0.382	0.337	0.791	0.791	0.209	0.000	3.108	1.180	5.14
318.15	0.442	0.292	0.369	0.339	0.803	0.803	0.197	0.000	3.041	1.154	5.14
318.55	0.588	0.377	0.264	0.359	0.833	0.833	0.167	0.000	2.408	1.340	3.49
318.95	0.618	0.394	0.243	0.363	0.849	0.849	0.151	0.000	2.314	1.288	3.47
320.05	0.740	0.459	0.162	0.379	0.899	0.899	0.101	0.000	2.016	1.233	3.12
320.85	0.806	0.494	0.119	0.387	0.910	0.910	0.090	0.000	1.843	1.430	2.43
322.55	0.901	0.542	0.060	0.398	0.952	0.952	0.048	0.000	1.654	1.402	2.18
325.35	1.000	0.590	0.000	0.410	1.000	1.000	0.000	0.000	1.444		
E/F = 3; 50.0 kPa											
349.55	0.000	0.000	0.473	0.527	0.000	0.000	1.000	0.000		1.125	
341.55	0.108	0.049	0.402	0.549	0.250	0.250	0.750	0.000	2.559	1.378	2.75
335.65	0.170	0.074	0.365	0.561	0.510	0.510	0.490	0.000	4.121	1.280	5.10
329.95	0.314	0.130	0.284	0.586	0.709	0.709	0.291	0.000	3.979	1.258	5.32
326.45	0.394	0.158	0.243	0.599	0.780	0.780	0.220	0.000	4.046	1.311	5.45
324.45	0.588	0.219	0.153	0.628	0.836	0.836	0.164	0.000	3.355	1.697	3.57
324.25	0.630	0.231	0.136	0.633	0.859	0.859	0.141	0.000	3.290	1.666	3.58
323.95	0.793	0.275	0.072	0.653	0.904	0.904	0.096	0.000	2.943	2.171	2.46
324.35	0.837	0.286	0.056	0.658	0.926	0.926	0.074	0.000	2.857	2.122	2.43
325.45	0.940	0.311	0.020	0.669	0.968	0.968	0.032	0.000	2.646	2.433	1.92
326.95	1.000	0.324	0.000	0.676	1.000	1.000	0.000	0.000	2.485		

[a] equilibrium temperature (T); mole fraction of liquid phase for n-hexane (guaiacol-free basis) (x_1'); mole fraction of vapor phase for n-hexane (guaiacol-free basis) (y_1'); mole fractions of liquid phase for n-hexane, ethanol, and guaiacol (x_1, x_2, and x_3); mole fractions of liquid phase for n-hexane, ethanol, and guaiacol (y_1, y_2, and y_3); activity coefficient of n-hexane and ethanol (γ_1 and γ_2); and relative volatility of n-hexane to ethanol (α_{12}).

[b] Expanded combined uncertainties (U) with $k = 2$ for $U(T)$ is 0.20 K, $U(P)$ is 0.2 kPa, and $U(x_1)$ and $U(y_1)$ are 0.006.

[c] y_3 are lower than 0.0005.

Table 3
The equation and parameters of the extended Antoine and the NIST Wagner 25[a].

Compounds	The extended Antoine [b]								
	A_1	A_2	A_3	A_4	A_5	10^6A_6	A_7	A_8	A_9
n-hexane	97.742	−6995.5	0	0	−12.702	12.381	2	177.83	507.6
ethanol	66.396	−7122.3	0	0	−7.142	2.885	2	159.05	514.0
guaiacol	244.642	−17,453.0	0	0	−33.723	19.843	2	31.5	423.9

	The NIST Wagner25[c]							
	A_1	A_2	A_3	A_4	$\ln P_{ci}$	T_{ci}	T_{lower}	T_{upper}
dimethyl isosorbide	−8.552	2.397	−4.204	−3.911	8.041	688	220	688

[a] Parameters of the extended Antoine and the NIST Wagner25 were retrieved from the Aspen Plus physical property databank.
[b] Equation (the extended Antoine): $\ln(P^{sat}) = A_1 + A_2/(T + A_3) + A_4T + A_5\ln T + A_6T^{A_7}$ for $A_8 < T < A_9$, where P^{sat} is in kPa and T in K.
[c] Equation (the NIST Wagner25): $\ln(P^s) = \ln P_{ci} + \frac{A_1(1-T_{ri}) + A_2(1-T_{ri})^{1.5} + A_3(1-T_{ri})^{2.5} + A_4(1-T_{ri})^5}{T_{ri}}$ for $T_{lower} \le T \le T_{upper}$, where P^s is in kPa, T in K, and $T_{ri} = T/T_{ci}$

$$\alpha_{12} = \frac{y_1/x_1'}{y_2/x_2'} \quad (2)$$

In this equation, the relative volatility of n-hexane to ethanol is represented by α_{12}, mole fractions of liquid phase for n-hexane and ethanol on an entrainer-free basis are denoted as x_1' and x_2', and mole fractions of vapor phase for n-hexane and ethanol are defined as y_1 and y_2. The VLE data in Tables 2 and 4 highlight important trends, including altered equilibrium temperatures, enhanced relative volatilities, and the removal of azeotropic constraints when entrainers are added to the mixture. These effects are visually depicted in Figs. 1–4.

Figs. 1 and 2 illustrate that the presence of guaiacol in the n-hexane and ethanol mixture exhibits a comparable effect to that of DMI. Both entrainers increase the equilibrium temperature when added at an E/F

Table 4
Experimental VLE data for pseudo-ternary mixture of n-hexane (1) + ethanol (2) + dimethyl isosorbide (3) [a,b,c].

T/K	x_1'	x_1	x_2	x_3	y_1'	y_1	y_2	y_3	γ_1	γ_2	α_{12}
E/F = 1; 100.0 kPa											
357.05	0.000	0.000	0.791	0.209	0.000	0.000	1.000	0.000		1.006	
350.85	0.051	0.040	0.744	0.216	0.195	0.195	0.805	0.000	3.668	1.095	4.51
346.25	0.109	0.084	0.691	0.225	0.364	0.364	0.636	0.000	3.726	1.119	4.69
339.85	0.209	0.160	0.602	0.238	0.605	0.605	0.395	0.000	3.989	1.042	5.78
337.95	0.370	0.275	0.466	0.259	0.680	0.680	0.320	0.000	2.766	1.184	3.61
337.05	0.516	0.373	0.350	0.277	0.719	0.719	0.281	0.000	2.216	1.440	2.40
337.15	0.569	0.408	0.309	0.283	0.733	0.733	0.267	0.000	2.062	1.541	2.08
337.35	0.701	0.492	0.210	0.298	0.775	0.775	0.225	0.000	1.797	1.894	1.47
339.45	0.835	0.573	0.114	0.313	0.835	0.835	0.165	0.000	1.553	2.344	1.00
341.15	0.878	0.598	0.084	0.318	0.868	0.868	0.132	0.000	1.467	2.347	0.91
344.45	0.967	0.650	0.022	0.328	0.963	0.963	0.037	0.000	1.350	2.186	0.89
347.25	1.000	0.669	0.000	0.331	1.000	1.000	0.000	0.000	1.252		
E/F = 1; 50.0 kPa											
339.25	0.000	0.000	0.791	0.209	0.000	0.000	1.000	0.000		1.030	
332.25	0.064	0.050	0.732	0.218	0.253	0.253	0.747	0.000	3.394	1.131	4.94
326.15	0.120	0.093	0.681	0.226	0.478	0.478	0.522	0.000	4.276	1.123	6.69
319.95	0.237	0.180	0.579	0.241	0.683	0.683	0.317	0.000	3.938	1.080	6.94
318.45	0.366	0.270	0.471	0.259	0.727	0.727	0.273	0.000	2.940	1.231	4.62
317.65	0.516	0.373	0.350	0.277	0.770	0.770	0.230	0.000	2.328	1.449	3.15
317.75	0.615	0.438	0.273	0.289	0.780	0.780	0.220	0.000	1.999	1.770	2.22
318.05	0.690	0.484	0.218	0.298	0.812	0.812	0.188	0.000	1.860	1.864	1.95
319.25	0.839	0.575	0.111	0.314	0.860	0.860	0.140	0.000	1.587	2.581	1.18
320.25	0.881	0.600	0.082	0.318	0.879	0.879	0.121	0.000	1.500	2.862	0.99
322.65	0.962	0.648	0.025	0.327	0.961	0.961	0.039	0.000	1.392	2.672	0.99
324.85	1.000	0.669	0.000	0.331	1.000	1.000	0.000	0.000	1.297		
E/F = 3; 50.0 kPa											
346.05	0.000	0.000	0.558	0.442	0.000	0.000	1.000	0.000		1.099	
341.85	0.046	0.025	0.523	0.452	0.099	0.099	0.901	0.000	1.953	1.257	2.30
336.75	0.116	0.062	0.472	0.466	0.252	0.252	0.748	0.000	2.360	1.439	2.56
329.85	0.243	0.124	0.386	0.490	0.587	0.587	0.413	0.000	3.458	1.322	4.43
325.85	0.358	0.176	0.314	0.510	0.717	0.717	0.283	0.000	3.417	1.340	4.53
323.45	0.561	0.257	0.201	0.542	0.802	0.802	0.198	0.000	2.844	1.636	3.17
323.45	0.645	0.288	0.159	0.553	0.844	0.844	0.156	0.000	2.671	1.641	2.97
323.45	0.694	0.305	0.134	0.561	0.867	0.867	0.133	0.000	2.590	1.641	2.88
324.45	0.861	0.360	0.059	0.581	0.925	0.925	0.075	0.000	2.261	2.025	1.99
324.85	0.914	0.377	0.035	0.588	0.958	0.958	0.042	0.000	2.204	1.862	2.14
327.35	1.000	0.403	0.000	0.597	1.000	1.000	0.000	0.000	1.975		

[a] equilibrium temperature (T); mole fraction of liquid phase for n-hexane (DMI-free basis) (x_1'); mole fraction of vapor phase for n-hexane (DMI-free basis) (y_1'); mole fractions of liquid phase for n-hexane, ethanol, and DMI (x_1, x_2, and x_3); mole fractions of liquid phase for n-hexane, ethanol, and DMI (y_1, y_2, and y_3); activity coefficient of n-hexane and ethanol (γ_1 and γ_2); and relative volatility of n-hexane to ethanol (α_{12}).
[b] Expanded combined uncertainties (U) with $k = 2$ for $U(T)$ is 0.20 K, $U(P)$ is 0.2 kPa, and $U(x_1)$ and $U(y_1)$ are 0.006.
[c] y_3 are lower than 0.0005.

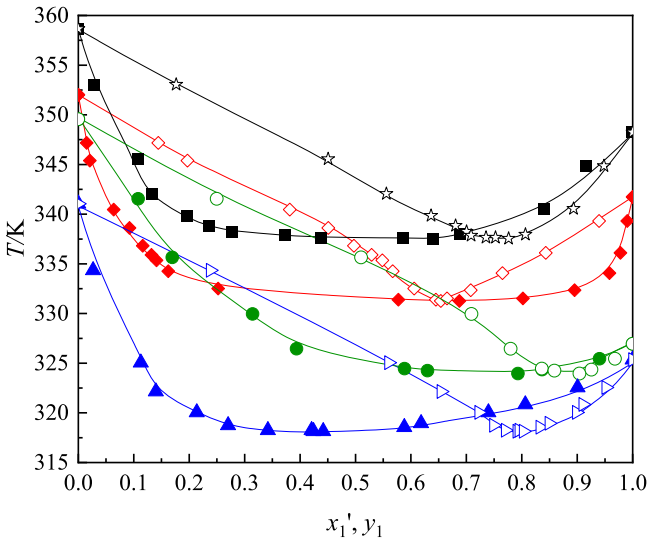

Fig. 1. x_1'-y_1-T profiles for n-hexane (1) + ethanol (2) + guaiacol (3). Experimental data with an E/F of 1: (black ■), x_1' and (black ☆), y_1 at 100.0 kPa; and (blue ▲), x_1' and (blue ▷), y_1 at 50.0 kPa; with an E/F of 3: (green ●), x_1' and (green ○), y_1 at 50.0 kPa; and binary mixture: (red ◆), x_1 and (red ◇), y_1 at 101.3 kPa. Correlated results from the NRTL model (——): with an E/F of 1, 100.0 kPa (black); and 50.0 kPa (blue); with an E/F of 3, 50.0 kPa (green); and (– · –), binary mixture at 101.3 kPa (red). The binary mixture were taken from our previous work [58]. Note: x_1 and y_1 denote the entrainer-free mole fractions of n-hexane in the liquid and vapor phases, respectively, as defined in Tables 2 and 4.

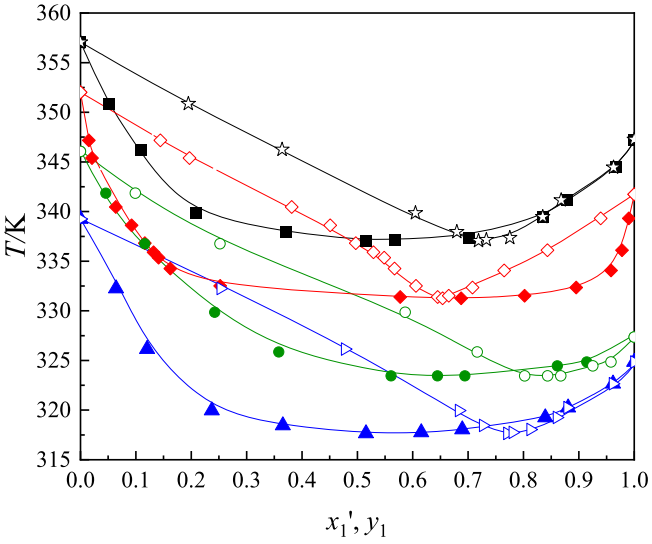

Fig. 2. x_1'-y_1-T profiles for n-hexane (1) + ethanol (2) + dimethyl isosorbide (3). Experimental data with an E/F of 1: (black ■), x_1' and (black ☆), y_1 at 100.0 kPa; and (blue ▲), x_1' and (blue ▷), y_1 at 50.0 kPa; E/F of 3: (green ●), x_1' and (green ○), y_1 at 50.0 kPa; and binary mixture: (red ◆), x_1 and (red ◇), y_1 at 101.3 kPa. Correlated results from the NRTL model (——): with an E/F of 1, 100.0 kPa (black); and 50.0 kPa (blue); with an E/F of 3, 50.0 kPa (green); and (– · –), binary mixture at 101.3 kPa (red). The binary mixture were taken from our previous work [58]. Note: x_1 and y_1 denote the entrainer-free mole fractions of n-hexane in the liquid and vapor phases, respectively, as defined in Tables 2 and 4.

of 1 and at a pressure of 100.0 kPa, compared to the binary mixture without an entrainer. Guaiacol and DMI demonstrate an affinity for

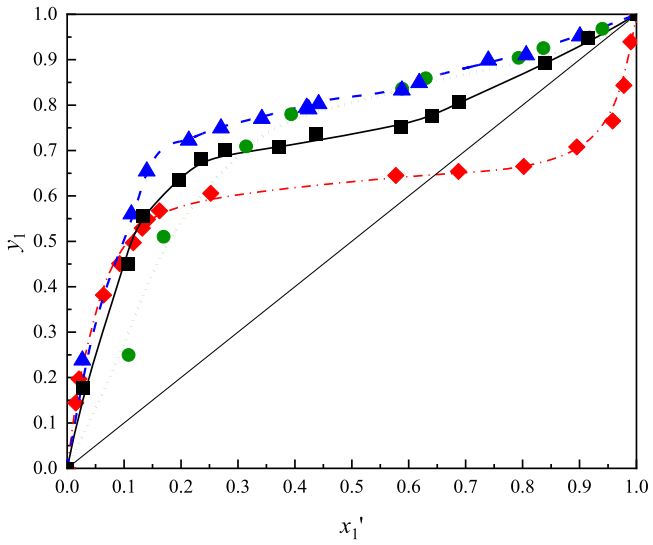

Fig. 3. x_1'-y_1 profiles for n-hexane (1) + ethanol (2) + guaiacol (3). Experimental data with an E/F of 1: (black ■), at 100.0 kPa; and (blue ▲), at 50.0 kPa; E/F of 3: (green ●), at 50.0 kPa; and (red ◆), binary mixture at 101.3 kPa. Correlated results from the NRTL model with an E/F of 1: (——), at 100.0 kPa (black); and (– – –), 50.0 kPa (blue); with an E/F of 3: (····), 50.0 kPa (green); and (– · –), binary mixture at 101.3 kPa (red). The binary mixture were taken from our previous work [58].

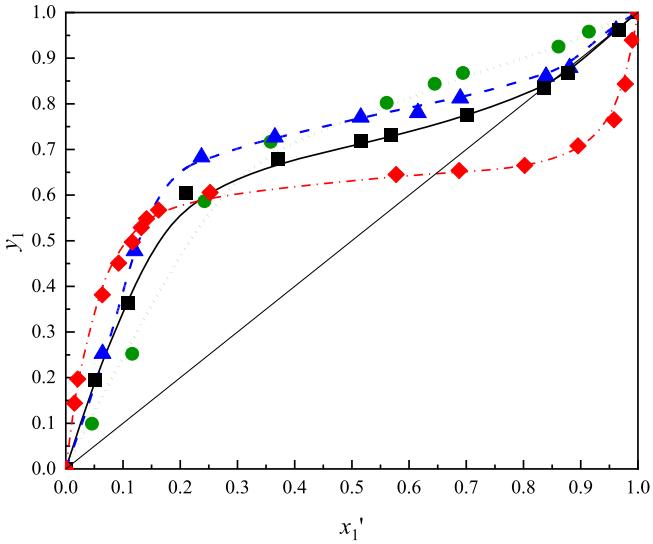

Fig. 4. x_1'-y_1 profiles for n-hexane (1) + ethanol (2) + dimethyl isosorbide (3). Experimental data with an E/F of 1: (black ■), at 100.0 kPa; and (blue ▲), at 50.0 kPa; with an E/F of 3: (green ●), at 50.0 kPa; and (red ◆), binary mixture at 101.3 kPa. Correlated results from the NRTL model with E/F of 1: (——), at 100.0 kPa (black); and (– – –), 50.0 kPa (blue); with an E/F of 3: (····), 50.0 kPa (green); and (– · –), binary mixture at 101.3 kPa (red). The binary mixture were taken from our previous work [58].

ethanol, which reduces the vaporization of ethanol. Moreover, the addition of a high boiling point entrainer in the mixture, with an E/F of 1 (or 50 % mass of the total liquid composition), significantly affects the boiling point of the mixture. As a result, these two factors contribute to an increase in the equilibrium temperature. The effects of reduced pressure were also investigated. Lowering the pressure from 100.0 to 50.0 kPa while maintaining a constant E/F of 1 lead to a significant decrease in the equilibrium temperature. This is because each

component has a lower boiling point under reduced pressure, requiring less heat to achieve equilibrium.

At the pressure of 50.0 kPa, increasing the amount of guaiacol and DMI to an E/F of 3 results in a higher equilibrium temperature compared to an E/F of 1. This is attributed to the entrainers becoming the major constituents of the liquid phase. Moreover, it reduces the vaporization of both n-hexane and ethanol, thereby elevating the equilibrium temperature. A minimum temperature is observed at all investigated E/Fs and pressures with the addition of guaiacol. However, this does not correspond to the presence of an azeotropic point, as the vapor phase composition of n-hexane consistently remains higher than its liquid phase composition. Similarly, in the presence of DMI, the minimum temperature does not indicate an azeotrope either. At an E/F of 3 and a pressure of 50.0 kPa, the vapor phase composition of n-hexane always exceeds that of the liquid phase. Furthermore, although an azeotrope occurs at an E/F of 1 and pressures of 50 and 100 kPa, the composition of this azeotrope differs from the composition at which the minimum temperature is observed. The occurrence of the minimum temperature in this system is predominantly governed by strong positive deviations from ideal behavior. These deviations are mainly associated with polarity differences and hydrogen-bonding effects that induce repulsive mixing, increasing activity coefficients. This phenomenon is accompanied by a depression of the boiling point, in which the total vapor pressure of the mixture surpasses that of pure components because of non-ideal interactions. Other contributing phenomena include ternary molecular interactions, where the introduction of guaiacol and DMI alters the n-hexane and ethanol binary interactions. Additionally, pressure dependence, where reduced pressure lowers the boiling points of all compounds, while changes in relative volatility accentuate non-ideality. Collectively, these phenomena elevate the total vapor pressure at specific compositions, resulting in a minimum boiling temperature, even if the azeotrope is significantly shifted or completely removed. This minimum temperature behavior is consistent with our previous studies of the n-hexane and ethanol mixture when 1-butylpyrrolidin-2-one (NBP) and NMP were used as entrainers [58]. This finding also aligns with the reported azeotropic mixtures from literature, such as those involving ethanol and methyl propionate and ethanol and 2-butanone with the addition of various ionic liquids as entrainers [15,59,60], as well as acetonitrile-water mixture with the presence of dimethyl sulfoxide and ethylene glycol [61,62].

In Figs. 1 and 2, the VLE curves are plotted in terms of the entrainer-free mole fractions x_1' and y_1. At high entrainer loadings, the strong non-ideal behavior and the re-normalization to an entrainer-free basis can lead to pronounced curvature of the x_1'-y_1 profiles and to sections where the projected vapor curve appears below the projected liquid curve in the 2D representation. This effect is purely geometric and does not indicate a violation of phase-equilibrium conditions, as confirmed by the Van Ness consistency test (Table 5) and the random distribution of residuals (Figs. S7-S8). Data points that visually overlap at high x_1' (particularly in Fig. 2) correspond to measurements at very similar compositions and temperatures; they were retained to demonstrate measurement reproducibility.

The x_1'-y_1 profiles, shown in Figs. 3 and 4, highlight how the presence of guaiacol and DMI contributes to the elimination of the azeotropic point in the n-hexane and ethanol mixture. The initial azeotropic composition was $x_1 = 0.660$ [58]. The addition of guaiacol and DMI to the mixture modifies its non-ideal thermodynamic behavior by affecting the molecular interactions of its components. Since ethanol is polar and n-hexane is non-polar, both guaiacol and DMI, which are polar components, demonstrate stronger interactions toward polar ethanol compared to non-polar n-hexane. This selective affinity weakens the ethanol and n-hexane interactions, thereby enhancing the relative volatility and removing the azeotropic point, which facilitates a more effective separation of n-hexane from ethanol. The pronounced affinity between ethanol and both guaiacol and DMI can be attributed to specific hydrogen-bonding interactions, wherein the hydroxyl group in ethanol acts as a hydrogen bond donor to the phenolic hydroxyl and ether oxygen in guaiacol, which serve as hydrogen bond acceptors. Similarly, the interactions of ethanol and DMI involve the hydroxyl group of ethanol bonding with ether oxygen in DMI. On the other hand, n-hexane, as a nonpolar compound, exhibits weaker van der Waals interactions with guaiacol and DMI.

With the addition of guaiacol, the VLE data presented in Table 2 shows that the activity coefficient of n-hexane (γ_1) is larger than that of ethanol (γ_2) across all compositions of n-hexane for the investigated E/Fs and pressures. This indicates a stronger molecular affinity between guaiacol and ethanol than between guaiacol and n-hexane, which enhances the volatility of n-hexane and effectively removes the azeotropic point. Notably, the azeotropic point has already been removed in the presence of guaiacol at an E/F of 1 and a pressure of 100.0 kPa. Additionally, this work studied the effect of lowering the pressure from 100.0 to 50.0 kPa at an E/F of 1 on relative volatility. Table 2 illustrates that the values of γ_2 at 50.0 kPa are overall smaller than at 100.0 kPa. This indicates that at a reduced pressure, the guaiacol and ethanol interaction is stronger. This enhanced interaction facilitates the easier separation of n-hexane, and therefore the relative volatility at a reduced pressure is significantly increased, as shown in Fig. 3.

This study further investigated the effect of the guaiacol amount added to the mixture. The addition of guaiacol to the mixture with an E/F of 3 was evaluated. Given that a significant increase in relative volatility is observed when the pressure is reduced from 100.0 to 50.0 kPa at an E/F of 1, the VLE measurements at an E/F of 3 were conducted at a pressure of 50.0 kPa to examine whether a further increase in guaiacol amount would amplify the separation of n-hexane from ethanol. As shown in Fig. 3, however, when the amount of the guaiacol is increased from an E/F of 1 to an E/F of 3 at a pressure of 50.0 kPa, the relative volatility remains unchanged. This behavior is attributed to the tendency of guaiacol, when presented in higher amounts, to interact not only with ethanol but also with itself. Although the interaction between guaiacol and ethanol is still present, as indicated by the γ_2 values being smaller than γ_1 across all n-hexane compositions, the self-interaction of guaiacol prevents the interaction between guaiacol and ethanol from being as effective as at an E/F of 1 and a pressure of 50.0 kPa. Consequently, the interaction strength between guaiacol and ethanol at an E/F of 3 is diminished compared to at an E/F of 1, under the same pressure of 50.0 kPa. This reduced interaction reflected by the higher values of γ_2 at an E/F of 3 compared to that at an E/F of 1 at the same pressure. Conversely, the non-ideality of n-hexane increases when a larger amount of guaiacol is added to the mixture. This can be explained by the fact that n-hexane, a non-polar compound, exhibits an easier tendency to evaporate when the liquid mixture is dominated by the polar guaiacol composition. This is indicated by the higher values of γ_1 at an E/F of 3 compared to an E/F of 1 at the same pressure of 50.0 kPa. At this pressure, although the γ_1 values increase, increasing the E/F from 1 to 3 does not lead to an increase in relative volatility, as this is accompanied by an increase in γ_2.

Unlike with the presence of guaiacol, where γ_2 values are consistently smaller than γ_1 across all investigated E/Fs and pressures throughout all n-hexane compositions, the presence of DMI shows a distinct behavior. As presented in Table 4, the VLE data with the

Table 5
Results of the thermodynamic consistency test.

Mixtures	Δy^a	ΔP^b	Results
n-hexane (1) + ethanol (2) + guaiacol (3)	0.5	0.8	Passed
n-hexane (1) + ethanol (2) + DMI (3)	0.5	0.9	Passed

[a] $\Delta y = \frac{1}{n_p} \times \sum_{i=1}^{n_p} \Delta y_i = \frac{1}{n_p} \times \sum_{i=1}^{n_p} 100|y_i^{cal} - y_i^{exp}| < 1$

[b] $\Delta P = \frac{1}{n_p} \times \sum_{i=1}^{n_p} \Delta P_i = \frac{1}{n_p} \times \sum_{i=1}^{n_p} 100|\frac{P_i^{cal} - P_i^{exp}}{P_i^{exp}}| < 1$

addition of DMI demonstrate that γ_2 values are smaller than γ_1 at the entire composition of n-hexane only at an E/F of 3 and a pressure of 50.0 kPa. This shows stronger molecular interactions between DMI and ethanol than between DMI and n-hexane. As a result, the relative volatility is significantly enhanced, allowing the azeotrope to be effectively removed under these conditions, as illustrated in Fig. 4. However, when DMI is added to the mixture at an E/F of 1 and pressures of 50.0 and 100.0 kPa, the γ_2 values, particularly, in the n-hexane-rich region, are higher than γ_1. This indicates insufficient interactions between DMI and ethanol in this region. As a result, although DMI can increase relative volatility, it does not completely remove the azeotrope but shifts its composition from the original azeotropic point at $x_1 = 0.660$ toward the n-hexane-rich region.

Fig. 4 presents that reducing the pressure from 100.0 to 50.0 kPa when DMI is added at an E/F of 1 does not significantly increase the relative volatility in the n-hexane-rich region, and the azeotrope remains present in the mixture. In contrast, when a larger quantity of DMI is added at an E/F of 3 and operated at a pressure of 50.0 kPa, the relative volatility can be significantly increased, and the azeotropic point is effectively eliminated. The different behaviors between guaiacol and DMI can be attributed to their polarity properties. DMI exhibits lower polarity than guaiacol, as reflected by its lower HSPs values, listed in Table S1 of the Supplementary File. This lower polarity characteristic reduces the potential of self-interaction between molecules of DMI compared to that of guaiacol. Therefore, adding a larger amount of DMI at a low pressure still allows for effective interactions between DMI and ethanol. Our earlier research applied unimolecular quantum chemical calculations through COSMO-RS to investigate the interaction tendencies of polar entrainers. It was observed that these entrainers form stronger interactions with molecules possessing greater polar characteristics [28].

Notably, guaiacol at an E/F of 1 and a pressure of 100.0 kPa is already effective at removing the azeotrope, while DMI requires higher E/F and lower operating pressure to achieve the same result. This indicates that guaiacol demonstrates better separation performance than DMI in the separation of n-hexane and ethanol. Additionally, Figs. 3 and 4 confirm that the azeotropic point is completely eliminated under all conditions studied involving guaiacol. For DMI, complete azeotrope removal occurs at an E/F of 3 and a pressure of 50 kPa. This is achieved despite the minimum temperature present in the mixture, as shown in Figs. 1 and 2. The composition dependence of the activity coefficients γ_1 and γ_2 is illustrated in Figs. S1-S4, which show γ_i versus entrainer-free mole fraction of n-hexane for all investigated E/F values and pressures. These plots highlight the pronounced positive deviations from ideality and confirm the stronger non-ideality of n-hexane compared to ethanol in the presence of both guaiacol and DMI. The corresponding excess Gibbs free energy (G^E/RT) as a function of composition is presented in Figs. S5–S6. The asymmetric G^E curves are consistent with the selective interactions between the entrainers and ethanol and provide direct insight into the thermodynamic basis for the observed shifts and removal of the azeotropic point.

A comparative assessment of guaiacol and DMI as biobased entrainers and NMP as a benchmark entrainer was conducted to evaluate how these entrainers effectively separate n-hexane from ethanol, particularly with respect to their ability to enhance the relative volatility. Fig. 5 shows that, in the n-hexane-rich region at 50.0 kPa, guaiacol at E/F = 1 and DMI at E/F = 3 provide relative volatilities that are 13–17 % lower than those achieved with NMP at E/F = 1 and 100.0 kPa. This lower relative volatility would translate into a higher minimum number of theoretical stages and/or higher reflux ratios in an extractive distillation column, increasing energy demand compared to a process using NMP. However, when these thermodynamic differences are considered together with the markedly lower toxicity, biobased origin, and absence of strict regulatory constraints for guaiacol and DMI, these entrainers, under suitable operating conditions, remain attractive candidates for greener process designs. Their performance is comparable to that of

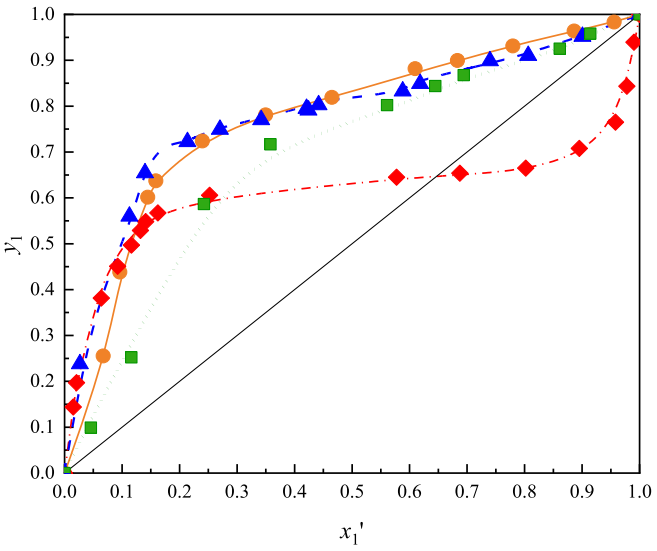

Fig. 5. x_1'-y_1 profiles for the comparison of the biobased entrainers guaiacol and DMI with the benchmark entrainer NMP in the n-hexane and ethanol mixture: (blue ▲), guaiacol with an E/F of 1 at 50.0 kPa; (green ■), DMI with an E/F of 3 at 50.0 kPa; (orange ●), NMP with an E/F of 1 at 100.0 kPa; ((red ◆), the binary mixture at 101.3 kPa, and regressed by NRTL: (– – –), blue line for guaiacol; (····), green line for DMI; (——), orange line for NMP; and (– · –), red line for the binary mixture. The binary mixture were taken from our previous work [58].

other green entrainers, such as NBP and selected ionic liquids, while avoiding the handling and miscibility challenges encountered with ionic liquids and deep eutectic solvents in this particular system.

In extractive distillation, a lower relative volatility at the same pressure and entrainer fraction generally increases the minimum number of theoretical stages and the energy demand through higher reflux ratios. Thus, the 13–17 % lower relative volatilities observed for guaiacol and DMI compared to NMP and NBP suggest that, at otherwise identical design assumptions, an extractive distillation column using guaiacol or DMI would require more separation effort. A detailed process simulation and optimization, including column configuration, heat integration, and entrainer recovery, is therefore needed to quantify the trade-off between increased energy consumption and the benefits arising from lower toxicity and improved sustainability of guaiacol and DMI. Such an analysis is beyond the scope of the present thermodynamic data study but represents an important direction for future work.

A direct comparison with our previous work on NBP and NMP as entrainers for n-hexane + ethanol [58] and a selected imidazolium ionic liquid [37] and glycerol-based deep eutectic solvents [39] is summarized in Fig. 6. At the azeotropic composition and 100.0 kPa, NMP at E/F = 1 yields the highest relative volatility among the green entrainers considered. At 50.0 kPa and E/F= 1, NBP exhibit the highest relative volatility between the green entrainers. Under the same pressure, guaiacol at E/F = 1 and DMI at E/F = 3 exhibit relative volatilities that are only 13–17 % lower than those of NBP, while still achieving complete removal of the azeotrope (guaiacol) or a strong shift with eventual removal (DMI at E/F = 3). In contrast, the benchmark solvent NMP at 100.0 kPa and E/F = 1 provides slightly higher relative volatilities but at the expense of significantly higher toxicity and regulatory restrictions. Thus, guaiacol and DMI bridge the gap between the high separation efficiency of NBP/NMP and the stricter safety requirements of modern solvent selection.

As summarized in Fig. 6, guaiacol at E/F = 1 and 50.0 kPa and DMI at E/F = 3 and 50.0 kPa provide relative volatilities only slightly lower than those of NBP and a selected imidazolium ionic liquid, but markedly higher than those reported for glycerol-based deep eutectic solvents in

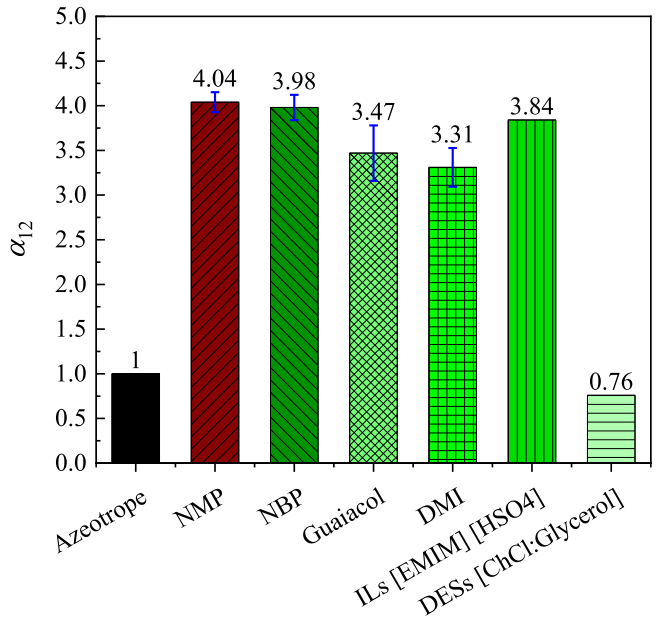

Fig. 6. Comparison for the relative volatility of n-hexane (1) to ethanol (2) (α_{12}) in the presence of conventional entrainer NMP (E/F= 1; 100.0 kPa) and various biobased and greener entrainers: NBP (E/F= 1; 50.0 kPa) [58]; guaiacol (E/F of 1; 50.0 kPa); DMI (E/F of 3; 50.0 kPa); 1-ethyl-3-methyl-imidazolium hydrogen sulfate [EMIM] [HSO_4] IL (E/F of 0.4; 101.3 kPa) [37]; ChCl:Glycerol (1:3) DES (E/F of 0.3, 328.15 K) [39]. All measurements were performed at the azeotropic composition.

the n-hexane + ethanol system. In addition, recent studies on DES entrainers for other azeotropic mixtures confirm that DESs often suffer from limited entrainer loading due to viscosity and miscibility constraints, which restrict the achievable relative volatility. This highlights that performance parity with NBP and ionic liquids, combined with superior practicality and greenness, is more relevant than achieving the highest absolute relative volatility.

Despite guaiacol and DMI exhibit slightly lower relative volatility compared to other entrainers, which could increase column stages and higher reflux ratios in extractive distillation, they still show practical potential as green entrainers in this process as both of them effectively increase the relative volatility and eliminate the azeotrope. While relative volatility is an important factor affecting separation efficiency, the values observed for guaiacol and DMI remain competitive for industrial applications, allowing for effective separation under optimized operating conditions. Importantly, both guaiacol and DMI are biobased entrainers that offer significant environmental advantages, such as non-toxic, biodegradable, and a renewable bio-based origin. In addition, guaiacol and DMI exhibit higher boiling points than NMP and do not experience the miscibility issues as ILs and DESs, when applied at high concentrations. These benefits make them attractive as entrainers in the context of sustainable process development. These characteristics compensate for their slightly reduced relative volatility compared to the benchmark entrainer, especially when considering the growing emphasis on greener solvents in regulatory and industrial frameworks. The results highlight the promising performance of guaiacol and DMI as biobased entrainers, positioning them as viable replacements for conventional entrainer NMP toward achieving greener and more sustainable extractive distillation processes.

While the favorable thermodynamic and separation performance of guaiacol and DMI establish them as promising green entrainers, it is important to note that these evaluations are primarily based on VLE data. Although these data provide an essential thermodynamic foundation for the effective design of extractive distillation processes. Their translation to real column design involves certain constraints. Specifically, these data do not incorporate the mass transfer resistance present at the vapor-liquid interfaces under actual operating conditions in a real column. Additionally, they assume a uniform entrainer concentration, which deviates from the reality where entrainer concentrations vary between different stages of the column. Therefore, to confirm their suitability for real-world extractive distillation applications, further validation of these entrainers is required. This should include rigorous process simulation or experimental validation of extractive distillation processes at the pilot-plant scale. In addition, a comprehensive assessment of total annual costs and sustainability should be conducted to ensure both economic and environmental feasibility.

3.2. Thermodynamic consistency test

The thermodynamic consistency test was performed to confirm the reliability of the VLE data. In this work, the Van Ness method, expressed in eqs. (3) and 4, was employed [52].

$$\Delta P = \frac{1}{n_p} \times \sum_{i=1}^{n_p} \Delta P_i = \frac{1}{n_p} \times \sum_{i=1}^{n_p} 100 \left| \frac{P_i^{cal} - P_i^{\exp}}{P_i^{\exp}} \right| \tag{3}$$

$$\Delta y = \frac{1}{n_p} \times \sum_{i=1}^{n_p} \Delta y_i = \frac{1}{n_p} \times \sum_{i=1}^{n_p} 100 \left| y_i^{cal} - y_i^{\exp} \right| \tag{4}$$

In these equations, n_p represents the number of data points, y is the vapor phase mole fraction, and P is the pressure. The term *cal* refers to the values calculated using the NRTL model, while *exp* refers to the values obtained from the experimental work. Under the criteria from the Van Ness method, the VLE data are regarded as thermodynamically consistent when the values for both ΔP and Δy are below 1. Table 5 illustrates that the values for ΔP and Δy for each pseudo-ternary mixture comply with this requirement. Additional details regarding the ΔP and Δy values can be found in Tables S2-S3 of the Supplementary File. Furthermore, the Van Ness test also requires that the residual distribution of the $\ln(\gamma_1/\gamma_2)$ exhibits a random pattern. Figures S7-S8 of the Supplementary File demonstrate that the residual distribution behaves randomly, providing further confirmation of the thermodynamic consistency of the investigated VLE data. In the original work of Van Ness, Legendre polynomials were suggested as a convenient flexible representation for the VLE data. In the present work, the NRTL model was instead used as the correlating function in the Van Ness test because NRTL is specifically developed for non-ideal and azeotropic mixtures and is widely applied for systems containing entrainers. Using NRTL at this stage also ensures consistency with the subsequent regression of the same VLE data. The small values of Δy and ΔP (Table 5) and the random distribution of residuals (Figs. S7-S8) confirm that the NRTL model is sufficiently flexible for the consistency test.

3.3. Regression of the VLE data

To determine the optimum BIPs, the VLE data were regressed using the NRTL model. Among the available excess-Gibbs-energy models, NRTL was selected because it is particularly suitable for strongly non-ideal mixtures with specific interactions, including systems with entrainers where local-composition effects are significant. Its application for the pseudo-ternary mixture with the presence of entrainer frequently results in strong correlations with the experimental data [35,63–68]. Previous work on pseudo-ternary mixtures of n-hexane and ethanol with NBP and NMP has demonstrated that NRTL correlates such systems accurately [58]. Moreover, we have previously reported that the NRTL model outperforms the UNIQUAC model based on their correlation results in the pseudo-ternary mixture that contains entrainers, particularly for methylcyclohexane – toluene with the presence of entrainer NMP and gamma-valerolactone [13]. For completeness, limited trial regressions with the Wilson and UNIQUAC models were performed for selected data sets. These models led to larger RMSDs in temperature and

compositions than NRTL, confirming that NRTL provides the best compromise between accuracy and parameter parsimony for the present pseudo-ternary mixtures. The equation for the model is outlined in eq. (5).

$$\ln\gamma_i = \frac{\sum_{j=1}^{n_c} x_j \tau_{ji} G_{ji}}{\sum_{k=1}^{n_c} x_k G_{ki}} + \sum_{j=1}^{n_c} \frac{x_j G_{ij}}{\sum_{k=1}^{N} x_k G_{kj}} \left(\tau_{ij} - \frac{\sum_{m=1}^{n_c} x_m \tau_{mj} G_{mj}}{\sum_{k=1}^{n_c} x_k G_{kj}} \right) \quad (5)$$

In the NRTL model equation, γ_i indicates the activity coefficient of the component i, and n_c defines the total number of components. In addition, the parameters associated with this model are described in eq. (6). The non-randomness constant for the binary pair interaction (i-j) in this model is denoted by C_{ij}.

$$G_{ij} = \exp(-C_{ij}\tau_{ij});\ \tau_{ij} = A_{ij} + B_{ij}/T;\ G_{ii} = 1;\ \tau_{ii} = 0 \quad (6)$$

For the n-hexane and ethanol pair, the BIPs were obtained from our previous study [58], which accurately represents the temperature range relevant to the VLE data in this work. For the n-hexane and ethanol binary mixture, the non-randomness constant was set at 0.47. On the other hand, this value was allowed to vary in the regression of the pseudo-ternary n-hexane-ethanol-guaiacol mixture, offering enhanced flexibility and leading to improved accuracy of the regression. However, for the mixture of n-hexane-ethanol-dimethyl isosorbide, the non-randomness constant was fixed at 0.30, as this provided better regression results. The Britt and Luecke method was used as a maximum likelihood-based algorithm to minimize the objective function (*OF*) in the regression, allowing determination of optimum BIPs [69]. The *OF* equation is presented in eq. (7). In this equation, n_p indicates the total number of data points, while σ refers to the standard deviations. Table 6 provides the optimum BIPs for the component pairs determined from the regression.

$$OF = \sum_{k=1}^{n_p} \left\{ \left| \frac{P_k^{cal} - P_k^{exp}}{\sigma_P} \right|^2 + \left| \frac{T_k^{cal} - T_k^{exp}}{\sigma_T} \right|^2 + \left| \frac{x_{1,k}^{cal} - x_{1,k}^{exp}}{\sigma_x} \right|^2 + \left| \frac{y_{1,k}^{cal} - y_{1,k}^{exp}}{\sigma_y} \right|^2 \right\} \quad (7)$$

The NRTL regression results demonstrated a strong agreement with the experimental VLE data for pseudo-ternary mixtures of n-hexane and ethanol containing guaiacol and DMI, respectively. The regression was conducted in a single regression for the VLE data across all E/Fs and pressures, resulting in BIPs that effectively capture the system's behavior across various compositions of the entrainer and pressures. The regression results for the n-hexane and ethanol mixture using guaiacol as an entrainer are presented in Fig. 1, while Fig. 2 illustrates the results with DMI as an entrainer. Moreover, Table 7 shows the root-mean-square deviations, confirming a strong correlation between the regressed values and the experimental data. Figures S9-S14 in the Supplementary File provide detailed residual plots for the mole fractions of both the liquid and vapor phases, as well as the temperature. These results affirm the reliability of the NRTL model and its associated BIPs for designing effective extractive distillation processes through a process simulation to separate the n-hexane and ethanol mixture using the biobased entrainers guaiacol and DMI.

Table 7
Root-Mean-Square Deviations (RMSD)[a].

	RMSD[b]			
	T/K	P/kPa	x_1'	y_1
n-hexane (1) + ethanol (2) + guaiacol (3)	0.38	0.6	0.006	0.007
n-hexane (1) + ethanol (2) + dimethyl isosorbide (3)	0.52	0.8	0.007	0.007

[a] T is a temperature, P is a pressure; x_1' is the mole fraction of liquid phase for n-hexane (entrainer-free basis), y_1: mole fraction of vapor phase for n-hexane.

[b] RMSD: $\Delta M = \sqrt{\frac{1}{n}\sum_{i=1}^{n} (M_{exp} - M_{cal})^2}$, where n represent the number of data points; M describes T, P, x_1', and y_1, respectively.

4. Conclusions

This study presents, for the first time, the VLE data for pseudo-mixtures of n-hexane-ethanol in the presence of the biobased entrainers guaiacol and DMI. The data were confirmed to be thermodynamically consistent, indicating their reliability. The results indicate that the introduction of guaiacol and DMI enhances the relative volatility of n-hexane to ethanol and effectively eliminates the azeotropic point. Introducing guaiacol to the n-hexane and ethanol mixture at an E/F of 1 and pressures of 50.0 and 100.0 kPa, as well as an E/F of 3 and a pressure of 50.0 kPa, effectively removes the azeotrope behavior. When DMI was added at an E/F of 1 and pressures of 50.0 and 100.0 kPa, the azeotropic point shifted significantly toward the n-hexane-rich region compared to the original azeotropic composition at $x_1 = 0.660$. However, the azeotrope is not completely eliminated. The azeotropic point is successfully removed when DMI was added at E/F of 3 and a pressure of 50 kPa.

Compared to our earlier results with NBP and NMP, guaiacol and DMI show somewhat lower relative volatilities but still provide effective azeotrope removal under optimal conditions. Guaiacol performs similarly to NBP at reduced pressure and moderate entrainer loadings, whereas DMI requires a higher E/F but benefits from lower self-association and good miscibility. These differences, together with the improved toxicological and sustainability profile of guaiacol and DMI, highlight the role of these solvents as competitive green alternatives to both NBP and NMP. In addition, at optimal operating conditions, guaiacol and DMI exhibit relative volatility performance comparable to the other greener entrainers such as NBP and IL and demonstrate better relative volatility than DES. These results highlight the viability of biobased solvents guaiacol and DMI as green entrainers, contributing to greener and more sustainable extractive distillation processes.

Furthermore, the NRTL model was employed to regress the VLE data, resulting in a good fit between the regressed values and the experimental data. As a result, optimum BIPs were successfully determined. The NRTL

Table 6
Binary interaction parameters from the NRTL model for pseudo-ternary mixtures of n-hexane (1) + ethanol (2) with the biobased entrainers guaiacol (3) and dimethyl isosorbide (3)[a,b].

i component	j component	A_{ij}	A_{ji}	B_{ij}/K	B_{ji}/K	C_{ij}
[c]n-hexane (1)	ethanol (2)	−10.342	−3.854	4120.934	1829.392	0.47
n-hexane (1)	guaiacol (3)	24.967	−14.786	−7227.525	4793.393	0.26
ethanol (2)	guaiacol (3)	11.866	−4.250	−1934.061	1244.481	0.55
n-hexane (1)	dimethyl isosorbide (3)	11.988	−12.067	−2984.570	3932.560	0.30
ethanol (2)	dimethyl isosorbide (3)	11.537	−11.680	−3369.973	3639.305	0.30

[a] A_{ij}, A_{ji}, B_{ij}, and B_{ji} are asymmetric parameters; C_{ij} is the non-randomness constant.
[b] NRTL: $.\tau_{ij} = A_{ij} + B_{ij}/T$
[c] The BIPs for the hexane (1) – ethanol (2) were obtained from our previous work [58].

model and its parameters obtained in this work provide a reliable thermodynamic basis for the process design of an extractive distillation process utilizing biobased entrainers guaiacol and DMI to separate n-hexane and ethanol. Future research will involve process simulations for the extractive distillation of n-hexane and ethanol mixture, with the presence of guaiacol and DMI to examine their separation performance under real-world column conditions. Additionally, the research will assess both economic viability and environmental sustainability.

CRediT authorship contribution statement

Dhoni Hartanto: Writing – original draft, Visualization, Software, Investigation, Data curation, Conceptualization. **Boelo Schuur:** Supervision, Resources, Methodology, Conceptualization. **Anton A. Kiss:** Writing – review & editing, Supervision, Project administration, Methodology, Conceptualization. **André B. de Haan:** Writing – review & editing, Supervision, Project administration, Funding acquisition, Conceptualization.

Declaration of competing interest

The authors declare that they have no known competing financial interests or personal relationships that could have appeared to influence the work reported in this paper.

Acknowledgements

The authors gratefully thank the Indonesia Endowment Fund for Education (LPDP)-Ministry of Finance of the Republic of Indonesia for providing the funding and the scholarship to Dhoni Hartanto (grant number SKPB-1597/LPDP/LPDP.3/2024).

Supplementary materials

Supplementary material associated with this article can be found, in the online version, at doi:10.1016/j.fluid.2026.114694.

Data availability

I have shared the data in the manuscript.

References

[1] J.A. Chavez Velasco, M. Tawarmalani, R. Agrawal, Systematic analysis reveals thermal separations are not necessarily most energy intensive, Joule 5 (2021) 330–343, https://doi.org/10.1016/j.joule.2020.12.002.
[2] A.B. de Haan, H.B. Eral, B. Schuur, Industrial Separation Processes, De Gruyter, 2025, https://doi.org/10.1515/9783111063812.
[3] D.S. Sholl, R.P. Lively, Seven chemical separations to change the world, Nature 532 (2016) 6–9.
[4] S.E. Demirel, J. Li, M.M.F. Hasan, Membrane separation process design and intensification, Ind. Eng. Chem. Res. 60 (2021) 7197–7217, https://doi.org/10.1021/acs.iecr.0c05072.
[5] M.K. Hadj-Kali, H.F. Hizaddin, I. Wazeer, L. El blidi, S. Mulyono, M.A. Hashim, Liquid-liquid separation of azeotropic mixtures of ethanol/alkanes using deep eutectic solvents: COSMO-RS prediction and experimental validation, Fluid Phase Equilib. 448 (2017) 105–115, https://doi.org/10.1016/j.fluid.2017.05.021.
[6] N.S. Muhammed, A.O. Gbadamosi, E.I. Epelle, A.A. Abdulrasheed, B. Haq, S. Patil, D. Al-Shehri, M.S. Kamal, Hydrogen production, transportation, utilization, and storage: recent advances towards sustainable energy, J. Energy Storage 73 (2023) 109207, https://doi.org/10.1016/j.est.2023.109207.
[7] J. Kang, S. He, W. Zhou, Z. Shen, Y. Li, M. Chen, Q. Zhang, Y. Wang, Single-pass transformation of syngas into ethanol with high selectivity by triple tandem catalysis, Nat. Commun. 11 (2020) 827, https://doi.org/10.1038/s41467-020-14672-8.
[8] J.G. Speight, Chapter 8 - hydrocarbons from synthesis gas. J.G.B.T.-H. of I.H.P. (Second E. Speight (Ed.), Gulf Professional Publishing, Boston, 2020, pp. 343–386, https://doi.org/10.1016/B978-0-12-809923-0.00008-4.
[9] H.M. Sbihi, I.A. Nehdi, S. Mokbli, M. Romdhani-Younes, S.I. Al-Resayes, Hexane and ethanol extracted seed oils and leaf essential compositions from two castor plant (Ricinus communis L.) varieties, Ind. Crops Prod. 122 (2018) 174–181, https://doi.org/10.1016/j.indcrop.2018.05.072.
[10] A.A. Kiss, J.-P. Lange, B. Schuur, D.W.F. Brilman, A.G.J. van der Ham, S.R. A. Kersten, Separation technology–Making a difference in biorefineries, Biomass and Bioenergy 95 (2016) 296–309, https://doi.org/10.1016/j.biombioe.2016.05.021.
[11] H.A. Kooijman, E. Sorensen, Recent advances and future perspectives on more sustainable and energy efficient distillation processes, Chem. Eng. Res. Des. 188 (2022) 473–482, https://doi.org/10.1016/j.cherd.2022.10.005.
[12] A.A. Kiss, Distillation technology – still young and full of breakthrough opportunities, J. Chem. Technol. Biotechnol. 89 (2014) 479–498, https://doi.org/10.1002/jctb.4262.
[13] D. Hartanto, B. Schuur, T. Schuttevaer, A.A. Kiss, A.B. de Haan, Isobaric vapor–Liquid equilibrium of methylcyclohexane + toluene with gamma-valerolactone as a biobased entrainer and 1-methylpyrrolidin-2-one as a conventional entrainer, J. Chem. Eng. Data 70 (2025) 1339–1351, https://doi.org/10.1021/acs.jced.4c00509.
[14] A.A. Kiss, Design, control and economics of distillation. Adv. Distill. Technol. Des. Control Appl., John Wiley & Sons, Inc., 2013, pp. 37–65, https://doi.org/10.1002/9781118543702.ch2.
[15] J. Zhu, Y. Sun, Y. Chen, N. Wu, R. Shi, Z. Ren, Q. Li, H. Zhao, Isobaric vapor–Liquid equilibrium experiments of methyl propionate + ethanol with different ionic liquids at 101.3 kPa, J. Chem. Eng. Data 70 (2025) 427–438, https://doi.org/10.1021/acs.jced.4c00517.
[16] V. Gerbaud, I. Rodriguez-Donis, in: A. Górak, Ž.B.T.-D. Olujić (Eds.), Chapter 6 - Extractive Distillation, Academic Press, Boston, 2014, pp. 201–245, https://doi.org/10.1016/B978-0-12-386878-7.00006-1.
[17] P.V. Tozzi, C.M. Wisniewski, N.J. Zalewski, M.J. Savelski, C.S. Slater, F.A. Richetti, Life cycle assessment of solvent extraction as a low-energy alternative to distillation for recovery of N-methyl-2-pyrrolidone from process waste, 7 (2018) 277–286. https://doi.org/10.1515/gps-2017-0030.
[18] J. Sherwood, T.J. Farmer, J.H. Clark, Catalyst: possible consequences of the N-methyl pyrrolidone REACH restriction, Chem 4 (2018) 2010–2012, https://doi.org/10.1016/j.chempr.2018.08.035.
[19] C.R. Kirman, B.R. Sonawane, J.G. Seed, N.O. Azu, W.T. Barranco, W.R. Hamilton, T.J. Stedeford, S.M. Hays, An evaluation of reproductive toxicity studies and data interpretation of N-methylpyrrolidone for risk assessment: an expert panel review, Regul. Toxicol. Pharmacol. 138 (2023) 105337, https://doi.org/10.1016/j.yrtph.2023.105337.
[20] D. Hartanto, B.S. Gupta, M. Taha, M.J. Lee, Isobaric vapour-liquid equilibrium of (tert-butanol + water) system with biological buffer TRIS at 101.3 kPa, J. Chem. Thermodyn. 98 (2016) 159–164, https://doi.org/10.1016/j.jct.2016.03.013.
[21] M. Taha, Designing new mass-separating agents based on piperazine-containing good's buffers for separation of propanols and water azeotropic mixtures using COSMO-RS method, Fluid Phase Equilib. 425 (2016) 40–46, https://doi.org/10.1016/j.fluid.2016.05.011.
[22] T. Brouwer, B. Schuur, Biobased entrainer screening for extractive distillation of acetone and diisopropyl ether, Sep. Purif. Technol. 270 (2021) 118749, https://doi.org/10.1016/j.seppur.2021.118749.
[23] T. Brouwer, B. Schuur, Bio-based solvents as entrainers for extractive distillation in aromatic/aliphatic and olefin/paraffin separation, Green Chem. 22 (2020) 5369–5375, https://doi.org/10.1039/D0GC01769H.
[24] W. Zhao, Q. Wu, L. Yang, Z. Wang, Y. Xu, Z. Zhu, P. Cui, Y. Wang, Process design, optimization and intensification for the efficient purification of the green solvent cyclopentyl methyl ether, Sep. Purif. Technol. 357 (2025) 130049, https://doi.org/10.1016/j.seppur.2024.130049.
[25] Q. Wang, P. Dai, A. Yang, W. Shen, J. Zhang, Deep learning-driven green solvent design and process intensification towards isopropyl alcohol-water azeotrope system, Sep. Purif. Technol. 360 (2025) 131103, https://doi.org/10.1016/j.seppur.2024.131103.
[26] J.P. Gomes, R. Silva, C.P. Nunes, D. Barbosa, Towards sustainable industrial processes: a preselection method for screening green solvents in the 1,3-butadiene extractive distillation process, Sustainability 17 (2025), https://doi.org/10.3390/su17083285.
[27] W. Wang, Y. Wang, W. Lu, W. Zhao, Z. Zhu, P. Cui, X. Li, X. Song, Experimental and mechanism study of separation of ethanol-ethyl tert-butyl ether with deep eutectic solvents based on molecular simulation, Sep. Purif. Technol. 359 (2025) 130587, https://doi.org/10.1016/j.seppur.2024.130587.
[28] D. Hartanto, B. Schuur, A.A. Kiss, A.B. de Haan, Effective selection of green organics and natural deep eutectic solvents as advanced entrainers by COSMO-RS and group contributions methods for enhanced design of extractive distillation, in: F. Manenti, G.V.B.T.-C.A.C.E. Reklaitis (Eds.), Comput. Aided Chem. Eng., Elsevier, 2024, pp. 1387–1392, https://doi.org/10.1016/B978-0-443-28824-1.50232-5.
[29] S.D. Rahayu, S. Altway, A.H. Tiwikrama, K. Kuswandi, Isobaric vapor–Liquid equilibria for separation of the n-propanol and water azeotropic system with the addition of a choline chloride–Ethylene glycol-based deep eutectic solvent as an entrainer, J. Chem. Eng. Data 70 (2025) 416–426, https://doi.org/10.1021/acs.jced.4c00511.
[30] Y. Peng, Y. Shen, J. Niu, X. Han, Separation of azeotropic mixture using a novel hybrid entrainer based on deep eutectic solvents, Fluid Phase Equilib. 592 (2025) 114326, https://doi.org/10.1016/j.fluid.2024.114326.
[31] K. Luo, C. Guo, J. Liang, Y. Gui, C. Gui, Energy and cost-efficient ionic liquids extractive distillation for producing electronic and polymer-grade propylene with emphasis on feedstock variability, Sep. Purif. Technol. 358 (2025) 130258, https://doi.org/10.1016/j.seppur.2024.130258.
[32] A. Iftakher, T. Leonard, M.M.F. Hasan, Integrating different fidelity models for process optimization: a case of equilibrium and rate-based extractive distillation

using ionic liquids, Comput. Chem. Eng. 192 (2025) 108890, https://doi.org/10.1016/j.compchemeng.2024.108890.
[33] Z. Zhang, B. Dong, Z. Zhang, J. Chen, H. Xin, Q. Zhang, Separation of acetonitrile + isopropanol azeotropic mixture using ionic liquids with acetate anion as entrainers, Fluid Phase Equilib. 521 (2020) 112725, https://doi.org/10.1016/j.fluid.2020.112725.
[34] A.A.A. Saif, A.A. Taimoor, S. Al-Shahrani, U. Saeed, S.-U. Rather, M.A. Alamoudi, Evaluating the ionic liquids, commercial solvents, and pressure-swing for efficient azeotropic separation, 20 (2025) 393–418. https://doi.org/10.1515/cppm-2024-0064.
[35] Y. Zhang, Z. Wang, X. Xu, J. Gao, D. Xu, L. Zhang, Y. Wang, Entrainers selection and vapour-liquid equilibrium measurements for separating azeotropic mixtures (ethanol + n-hexane/cyclohexane) by extractive distillation, J. Chem. Thermodyn. 144 (2020) 106070, https://doi.org/10.1016/j.jct.2020.106070.
[36] E. Gonzalez, J. Ortega, Densities and isobaric vapor-liquid equilibria of butyl esters (Methanoate to Butanoate) with ethanol at 101.32 kPa, J. Chem. Eng. Data 40 (1995) 1178–1183, https://doi.org/10.1021/je00022a004.
[37] Y. Wang, R. Hu, W. Liu, Z. Zhu, Y. Wang, J. Yang, J. Qi, P. Cui, Separation of ethanol/n-hexane azeotrope by imidazolium ionic liquids: experimental study and mechanism analysis, Sep. Purif. Technol. 357 (2025) 130063, https://doi.org/10.1016/j.seppur.2024.130063.
[38] A. Sander, A. Petračić, M. Rogošić, M. Župan, L. Frljak, M. Cvetnić, Feasibility of different methods for separating n-hexane and ethanol, Separations 11 (2024), https://doi.org/10.3390/separations11050151.
[39] A. Sharma, B.-S. Lee, H.Y. Shin, Assessing suitability of glycerol-derived green solvent for the separation of n-hexane + ethanol azeotropic mixture, accompanied by VLE studies using machine learning, J. Mol. Liq. 423 (2025) 127003, https://doi.org/10.1016/j.molliq.2025.127003.
[40] Y. Wang, H. Xu, Q. Yang, W. Wang, H. Li, Y. Wang, Z. Zhu, X. Li, X. Song, P. Cui, A novel intermediate heat exchange intensified extractive pressure-swing distillation process for efficiently separating n-hexane-tetrahydrofuran-ethanol, Chem. Eng. Sci. 300 (2024) 120593, https://doi.org/10.1016/j.ces.2024.120593.
[41] European Chemical Agency, 1,4:3,6-dianhydro-2,5-di-O-methyl-D-glucitol, (2017). https://chem.echa.europa.eu/100.023.782/overview?searchText=1,4:3,6-dianhydro-2,5-di-O-methyl-D-gluc (accessed July 3, 2025).
[42] A. Severini, C. Ferrari, A. Marchetti, F. Vizza, M. Bonechi, M. Innocenti, V. Lagostina, E. Salvadori, M. Chiesa, F. Roncaglia, C. Fontanesi, Electrochemical oxidation of guaiacol as a sacrificial anodic process producing fine chemical derivative, for hydrogen production via electrolysis, Int. J. Hydrogen Energy 124 (2025) 345–354, https://doi.org/10.1016/j.ijhydene.2025.03.439.
[43] K. van der Maas, D.H. Weinland, R.-J. van Putten, B. Wang, G.-J.M. Gruter, Catalyst free PET and PEF polyesters using a new traceless oxalate chain extender, Green Chem 26 (2024) 11182–11195, https://doi.org/10.1039/D4GC02791D.
[44] European Chemical Agency, Guaiacol, (2020). https://chem.echa.europa.eu/100.001.786/overview?searchText=guaiacol (accessed July 3, 2025).
[45] J.J. Bozell, G.R. Petersen, Technology development for the production of biobased products from biorefinery carbohydrates—The US Department of Energy's "Top 10" revisited, Green Chem. 12 (2010) 539–554, https://doi.org/10.1039/B922014C.
[46] F. Gao, R. Bai, F. Ferlin, L. Vaccaro, M. Li, Y. Gu, Replacement strategies for non-green dipolar aprotic solvents, Green Chem. 22 (2020) 6240–6257, https://doi.org/10.1039/D0GC02149K.
[47] Public report, 2-pyrrolidinone, 1-butyl-, 2020. https://www.industrialchemicals.gov.au/sites/default/files/STD1698publicreport%5B780KB%5Dpdf.
[48] R.C... Weast, J.G. Grasselli, Handbook of Data on Organic Compounds, 2nd Editon, CRC Press, Inc., Boca Raton, FL, 1989.
[49] H. Kim, N.R. Vinueza, S.S. Kelley, S. Park, Correlation between solubility parameters and recovery of phenolic compounds from fast pyrolysis bio-oil by diesel extraction, Carbon Resour. Convers. 1 (2018) 238–244, https://doi.org/10.1016/j.crcon.2018.08.004.
[50] A. Benazzouz, L. Moity, C. Pierlot, M. Sergent, V. Molinier, J.-M. Aubry, Selection of a greener set of solvents evenly spread in the Hansen space by space-filling design, Ind. Eng. Chem. Res. 52 (2013) 16585–16597, https://doi.org/10.1021/ie402410w.
[51] O. Buken, K. Mancini, A. Sarkar, A sustainable approach to cathode delamination using a green solvent, RSC Adv. 11 (2021) 27356–27368, https://doi.org/10.1039/D1RA04922D.
[52] H.C. Van Ness, Thermodynamics in the treatment of vapor/liquid equilibrium (VLE) data, 67 (1995) 859–872. https://doi.org/10.1351/pac199567060859.
[53] H. Renon, J. Prausnitz, Local compositions in thermodynamic excess functions for liquid mixtures, AIChE J. 14 (1968) 135–144, https://doi.org/10.1002/aic.690140124.
[54] T.P.V.B. Dias, L.A.A.P. Fonseca, M.C. Ruiz, F.R.M. Batista, E.A.C. Batista, A.J. A. Meirelles, Vapor–Liquid equilibrium of mixtures containing the following higher alcohols: 2-propanol, 2-methyl-1-propanol, and 3-methyl-1-butanol, J. Chem. Eng. Data 59 (2014) 659–665, https://doi.org/10.1021/je400581e.
[55] H. Keestra, T. Brouwer, B. Schuur, J.-P. Lange, Entrainer selection for the extractive distillation of acrylic acid and propionic acid, Chem. Eng. Res. Des. 192 (2023) 653–663, https://doi.org/10.1016/j.cherd.2023.02.049.
[56] Taylor, Barry N, C.E. Kuyatt, NIST Technical Note 1297 guidelines for evaluating and expressing the uncertainty of NIST measurement results, technology (1994).
[57] Evaluation of measurement data — Guide to the expression of uncertainty in measurement, 2008. https://www.bipm.org/documents/20126/2071204/JCGM_100_2008_E.pdf.
[58] D. Hartanto, B. Schuur, A.A. Kiss, A.B. de Haan, Isobaric vapor-liquid equilibrium of the azeotropic mixture n-hexane + ethanol with 1-butylpyrrolidin-2-one as a greener entrainer and 1-methylpyrrolidin-2-one as a benchmark entrainer, J. Chem. Eng. Data 70 (2025) 4091–4104, https://doi.org/10.1021/acs.jced.5c00445.
[59] W. Li, X. Chen, H. Yin, L. Li, T. Zhang, Isobaric vapor–Liquid equilibrium for 2-butanone + ethanol system containing different ionic liquids at 101.3 kPa, J. Chem. Eng. Data 63 (2018) 380–388, https://doi.org/10.1021/acs.jced.7b00783.
[60] W. Li, L. Li, L. Zhang, H. Li, T. Zhang, Isobaric vapor-liquid equilibrium for 2-butanone + ethanol + phosphate-based ionic liquids at 101.3 kPa, Fluid Phase Equilib. 456 (2018) 57–64, https://doi.org/10.1016/j.fluid.2017.10.001.
[61] Z. Zhang, M. Lv, D. Huang, P. Jia, D. Sun, W. Li, Isobaric vapor–Liquid equilibrium for the extractive distillation of acetonitrile + water mixtures using dimethyl sulfoxide at 101.3 kPa, J. Chem. Eng. Data 58 (2013) 3364–3369, https://doi.org/10.1021/je400531a.
[62] L. Zhang, D. Shen, Z. Zhang, X. Wu, Experimental measurement and modeling of vapor–Liquid equilibrium for the ternary system water + acetonitrile + ethylene glycol, J. Chem. Eng. Data 62 (2017) 1725–1731, https://doi.org/10.1021/acs.jced.7b00178.
[63] F. Li, M. Li, J. Guo, X. Hu, J. Zhu, Q. Li, H. Zhao, Isobaric vapor–Liquid equilibrium experiment of N-propanol and N-propyl acetate at 101.3 kPa, J. Chem. Eng. Data 68 (2023) 358–365, https://doi.org/10.1021/acs.jced.2c00609.
[64] M. Cao, H. Tian, M. Li, Vapor–Liquid equilibrium data determination and model correlation for 1-octene + 1,4-dioxane, 2-octanol + 1,4-dioxane, 1-octene + isophorone, and 2-octanol + isophorone systems at 101.3 kPa, J. Chem. Eng. Data 68 (2023) 2275–2282, https://doi.org/10.1021/acs.jced.3c00136.
[65] Z. Lei, W. Arlt, P. Wasserscheid, Selection of entrainers in the 1-hexene/n-hexane system with a limited solubility, Fluid Phase Equilib. 260 (2007) 29–35, https://doi.org/10.1016/j.fluid.2006.06.009.
[66] Z. Zhang, Z. Zhang, B. Dong, J. Chen, H. Xin, Q. Zhang, Vapor-liquid equilibrium experiment and model prediction for separating ethyl propionate and ethanol using ionic liquids with acetate anion, J. Mol. Liq. 318 (2020) 113688, https://doi.org/10.1016/j.molliq.2020.113688.
[67] C. Yang, H. Zeng, X. Yin, S. Ma, F. Sun, Y. Li, J. Li, Measurement of (vapor+liquid) equilibrium for the systems {methanol+dimethyl carbonate} and {methanol+dimethyl carbonate+tetramethylammonium bicarbonate} at p=(34.43, 67.74)kPa, J. Chem. Thermodyn. 53 (2012) 158–166, https://doi.org/10.1016/j.jct.2012.05.002.
[68] S. He, W. Fan, H. Huang, J. Gao, D. Xu, Y. Ma, L. Zhang, Y. Wang, Separation of the azeotropic mixture methanol and toluene using extractive distillation: entrainer determination, vapor–Liquid equilibrium measurement, and modeling, ACS Omega 6 (2021) 34736–34743, https://doi.org/10.1021/acsomega.1c05164.
[69] H.I. Britt, R.H. Luecke, The estimation of parameters in nonlinear, implicit models, Technometrics 15 (1973) 233–247, https://doi.org/10.2307/1266984.